The Astronomical Journal, 125:1689–1695, 2003 April

HIGH-REDSHIFT X-RAY–SELECTED QUASARS: CXOCY J125304.0−090737 JOINS THE CLUB[1]

Francisco J. Castander,[2,3,4,5] Ezequiel Treister,[2,3] Thomas J. Maccarone,[6] Paolo S. Coppi,[2] José Maza,[3] Stephen E. Zepf,[7] and Rafael Guzmán[8]

Received 2002 November 1; accepted 2002 December 26

ABSTRACT

We present a new X-ray–selected high-redshift quasar CXOCY J125304.0−090737 at $z = 4.179$, discovered by the Calán-Yale Deep Extragalactic Research (CYDER) Survey. This quasar is the fifth X-ray–selected high-redshift radio-quiet quasar ($z > 4$) found so far. Here we present its observed properties, which are characterized by its relative optical and X-ray faintness, its X-ray hardness, and its X-ray strength compared with optically selected quasars at high redshift. We also compare the X-ray–selected high-redshift radio-quiet quasars with their optically selected counterparts. We find that the optical to X-ray spectral slope, α_{ox}, is statistically harder (more X-ray luminous) for the X-ray–selected radio-quiet quasars than for the optically selected ones. This result, given the different range of rest frame ultraviolet luminosities studied and the selection of the samples, is consistent with the previously found correlation between X-ray and rest-frame ultraviolet luminosities and would extend that result to a much wider luminosity range at high redshift. Finally, we discuss the prospects of unveiling the quasar luminosity function at high redshifts using X-ray surveys. The discovery of a high-redshift object in the first field of our survey program provides suggestive evidence that X-ray–selected surveys may identify more such objects than would be expected from an extrapolation of the optical luminosity function.

Key words: galaxies: active — quasars: individual (CXOCY J125304.0−090737) — X-rays

1. INTRODUCTION

The formation of the first structures in the universe is one of the most interesting subjects in today's astronomy. Because quasars are intrinsically very luminous, they can be observed up to very high redshift and can therefore probe early epochs in the universe. Recent observations have found considerable numbers of quasars at high redshift (Anderson et al. 2001; Schneider et al. 2002), with some quasars being at redshifts ∼6 (Fan et al. 2001b), when the universe was less than 1 Gyr old.

The earliest quasar surveys were performed in the radio (e.g., Edge et al. 1959; Bennett 1962; Schmidt 1963) and the optical (e.g., Sandage 1965). While radio surveys have continued (e.g., White et al. 2000), in recent years greater attention has been placed on optical and X-ray surveys. Optical surveys are efficient finding quasars, as they can search large areas of the sky in reasonable amounts of time. At high redshift (in this paper meaning redshifts $z > 4$) the Sloan Digital Sky Survey (SDSS; York et al. 2000) has been very successful identifying quasars, and now there are more than 100 SDSS high-redshift quasars known (Anderson et al. 2001). However, most of those quasars have been selected based on their color properties and therefore may be biased against quasars with different photometric properties, such as heavily obscured ones. Recent studies suggest that this bias may not be too problematic though (Richards et al. 2003).

The other main quasar selection technique is X-ray detection, as X-ray emission appears to be a universal characteristic of quasars at all observed redshifts (Kaspi et al. 2000). However, given the relative faintness of the majority of the sources, X-ray surveys need to rely on optical spectroscopy for most of the identifications. The lack of spatial resolution of past X-ray missions made these efforts laborious so far. However, the *Chandra* X-ray satellite, with its superb angular resolution, has made the optical identification process much more efficient. The nature of the X-ray emission also ensures that the optical selection biases due to obscuration are strongly reduced (although the X-ray selection may introduce biases of its own). This is especially true at high redshift, where the observed X-ray photons were emitted at higher energies and can penetrate even considerable amounts of obscuring material.

At high redshifts ($z > 4$) there are only five known quasars selected by their X-ray emission. Three of them were found with the *ROSAT* satellite (Henry et al. 1994; Zickgraf et al. 1997; Schneider et al. 1998). The other two were detected by *Chandra* (Silverman et al. 2002; Barger et al. 2002). All of them are radio quiet except one (Zickgraf et al. 1997). There is another active galactic nucleus (AGN) detected at $z = 4.14$ in the *Chandra* Deep Field North (Barger et al. 2002). However, this source is optically faint, $M_B = -21.7 + 5 \times \log(h_{65})$, and therefore it is hard to estimate the contribution of the active nucleus itself and its putative host galaxy to the observed optical luminosity. We therefore exclude this object from further discussions. There is also an optically faint radio-loud AGN at $z = 4.42$ in the *Chandra* Deep Field North (Brandt et al. 2001; Vignali et al.

[1] Partly based on observations collected at the European Southern Observatory, Chile, under program 68.A-0459.

[2] Department of Astronomy, Yale University, P.O. Box 208101, New Haven, CT 06520.

[3] Departamento de Astronomía, Universidad de Chile, Casilla 36-D, Santiago, Chile.

[4] Andes Prize Fellow.

[5] Current address: Institut d'Estudis Espacials de Catalunya/CSIC, Gran Capità 2-4, E-08034 Barcelona, Spain.

[6] SISSA, via Beirut 2-4, I-34014 Trieste, Italy.

[7] Department of Physics and Astronomy, Michigan State University, East Lansing, MI 48824.

[8] Department of Astronomy, University of Florida, P.O. Box 112055, Gainesville, FL 32611.

2002a), but this object was selected in the radio. In total there are 56 AGNs[9] detected in X-rays at $z > 4$,[10] seven of which are radio-loud quasars, two of which are low-luminosity AGNs (one of these is radio loud), and twelve of which have not appeared in the literature so far. The remaining 36 sources are radio-quiet quasars and will be the sample we will discuss in this paper. Thirty-two were optically selected, and four X-ray selected. Twenty-six were detected by *Chandra*, nine by *ROSAT*, and one by *XMM-Newton*. These 36 sources have typical absorption-corrected X-ray fluxes between 10^{-15} and 3×10^{-14} ergs cm^{-2} s^{-1} in the 0.5–2.0 keV band. The absolute magnitudes of the optically selected quasars range from $M_B \sim -26$ to $-30 + 5 \times \log(h_{65})$, while the X-ray–selected quasars range from $M_B \sim -23$ to $-27 + 5 \times \log(h_{65})$. Thus, the high-redshift X-ray–selected quasars sample a different range of the optical luminosity function than the optically selected ones.[11]

There have been several studies of high-redshift optically selected quasars detected in X-rays (e.g., Kaspi et al. 2000; Vignali et al. 2001; Brandt et al. 2002a, 2002b; Bechtold et al. 2002; Vignali et al. 2002d, 2002a). The overall properties of the high-redshift population are similar to the low-redshift quasars (Kaspi et al. 2000; Vignali et al. 2002d). The X-ray spectral slope appears to be similar, $\Gamma \sim 2.0$, at low and high redshift (e.g., Vignali et al. 2002c, 2002d), although in some high-redshift cases it is harder (Bechtold et al. 2002). The optical to X-ray spectral index, α_{ox}, nonetheless appears to be steeper (optically stronger and/or X-ray weaker) at high redshift than locally (Vignali et al. 2001; Bechtold et al. 2002), although this trend may only be a result of the possible correlation of the optical to X-ray spectral index with optical luminosity. Vignali et al. (2002b), studying a sample of SDSS Early Data Release quasars, find that α_{ox} is correlated with rest-frame ultraviolet (UV) luminosity but does not depend significantly on redshift. They also find a correlation (with a slope different than unity) between X-ray and rest-frame UV luminosities (see also references therein).

Here we present the discovery of CXOCY J125304.0−090737, a $z = 4.179$ quasar selected in X-rays from *Chandra* archival images. Optical follow-up images were taken with the CTIO 4 m telescope, and the confirming optical spectrum was obtained with FORS2 on VLT. These observations were taken as part of the Calán-Yale Deep Extragalactic Research (CYDER) Survey (Castander et al. 2003; Treister & Castander 2003). The CYDER survey is a deep optical and near-infrared imaging and spectroscopic program encompassing several scientific goals. One of the key aims is the characterization of the population of faint X-ray sources. Therefore, some of the fields of the CYDER survey were selected to overlap with deep *Chandra* pointings.

In § 2 we describe the X-ray, optical, and near-infrared observations that lead to the discovery of CXOCY J125304.0−090737, presenting the data reduction procedures followed. In § 3 we discuss the observed characteristics of CXOCY J125304.0−090737 and compare them with those of the high-redshift population of radio-quiet quasars. We also discuss the differences between the X-ray and optically selected high-redshift QSOs. Finally, we present our conclusions in § 4.

Throughout we assume $H_0 = 65\ h_{65}$ km s^{-1} Mpc^{-1}, $\Omega_0 = 0.3$, and $\Omega_\Lambda = 0.7$. We define the photon index Γ as the exponent giving a photon flux density X-ray spectrum $f(E) \propto E^{-\Gamma}$ in photons cm^{-2} s^{-1} keV^{-1}.

2. OBSERVATIONS AND DATA ANALYSIS

2.1. *X-Ray Data*

The first X-ray field studied by the CYDER survey in the southern hemisphere was the *Chandra* pointing toward the Hickson group of galaxies HCG 62 centered on (J2000.0) $\alpha = 12^h53^m05^s.70$, $\delta = -09^\circ12'20''.0$ (PI: J. Vrtilek). This field was observed on 2000 January 25 with the ACIS-S detector configuration for a total 49.15 ks. We retrieved this image from the archive and analyzed it, using standard techniques with the CIAO package.

We remove bad columns and pixels using the guidelines specified on the ACIS Recipes,[12] and we remove flaring pixels using the FLAGFLARE routine. We use the full set of standard event grades (0, 2, 3, 4, 6) and create two images, one from 0.5 to 2.0 keV and one from 2.0 to 8.0 keV. We then use the WAVDETECT routine from the CIAO package to identify the point sources within these images, checking all wavelet scales from 1 to 16, separated by factors of 2. We detect 30 sources from 0.5–2.0 keV and 19 from 2.0–8.0 keV (with 15 detected in both bands, so that a total of 34 sources are detected) in the S3 ACIS CCD. We then use the PSEXTRACT script to extract spectra for these sources and provide a response matrix. CXOCY J125304.0−090737 was detected in both bands. Figure 2 shows a $30'' \times 30''$ cutout region centered on CXOCY J125304.0−090737 of the total (0.5–8.0 keV) band adaptively smoothed X-ray image. The total number of background-subtracted photons detected were 17.1 ± 4.2 in the soft (0.5–2.0 keV) band and 8.3 ± 3.0 in the hard (2.0–8.0 keV) band. This analysis will focus on CXOCY J125304.0−090737; the sample as a whole will be discussed in a future work.

We then fit the spectrum for CXOCY J125304.0−090737 in XSPEC 11.0 with a power-law model. We find a best-fitting photon power-law index of $1.57^{+0.39}_{-0.33}$ with no absorption and of $1.69^{+0.40}_{-0.35}$ (1 σ errors for the spectral indices) when the Galactic neutral hydrogen column of 3×10^{20} (as calculated using the HEASARC NH tool) is accounted for. These fits are done with three spectral channels, from 0.5–8.0 keV, which all suffer from statistics too poor for conventional χ^2 fitting, and the resulting values of χ^2 are close to zero, indicating that the bins have too few photons. Still, the same results are obtained when either the C statistic or the χ^2 statistic is used, so they can be considered to be as robust as any spectral fits based on less than 30 photons. The

[9] Here AGNs are defined in a broad sense, including quasars and active galaxies.

[10] See the excellent Web site http://www.astro.psu.edu/users/niel/papers/highz-xray-detected.dat maintained by Niel Brandt and Christian Vignali for a list of the high-redshift AGN detected in X-rays so far.

[11] Whenever we talk about optical magnitudes or luminosities, we do it in a broad sense, including optical and ultraviolet. The magnitudes in the observed frame are measured in the optical; however, they correspond to rest-frame ultraviolet absolute magnitudes or luminosities.

[12] See Clean the Data at http://www.astro.psu.edu/xray/acis/recipes/clean.html.

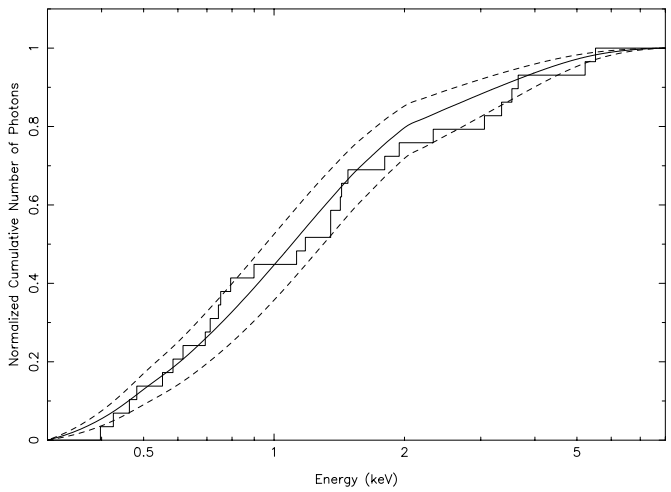

FIG. 1.—Observed cumulative X-ray photon energy distribution. The best-fitting power-law model is overplotted as a solid line, together with the 1 σ deviations (*dashed lines*).

0.5–8.0 keV Galactic absorption–corrected observed flux is $4.9 \pm 1.4 \times 10^{-15}$ ergs s^{-1} cm^{-2} with either model. Figure 1 shows the observed cumulative energy distribution.

2.2. *Optical and Near-Infrared Imaging Data*

As part of the CYDER survey we obtained V and I images of this field with the CTIO 4 m MOSAIC-II camera. The total integration time was 80 minutes in V and 25 minutes in I under 1.″1 seeing conditions. Images were reduced using standard techniques with the IRAF/MSCRED package.[13] We search for optical counterparts of our X-ray detections in the resulting images. The source matching is relatively simple, given the good spatial resolution of *Chandra*. Using the brightest nine point sources in the optical, we find an overall offset between the X-rays and the optical (tied to the USNO reference frame) of ΔR.A. $= 0.''9$ and Δdecl. $= 1.''0$ (see Castander et al. 2003 for further details). There is only one detectable optical counterpart within the error circle of the X-ray source CXOCY J125304.0−090737 down to our magnitude limit ($V < 25.8$ and $I < 23.8$ at 5 σ). The offset between the X-ray and optical centroids is 1.″3. For this object we performed PSF-fitting photometry measuring $V = 23.65 \pm 0.05$ and $I = 22.52 \pm 0.08$. Image cutouts of this object are shown in Figure 2.

Near-infrared data for this field were obtained at LCO using the du Pont 2.5 m telescope with the Wide Field Infrared Camera. The total integration time was 62 minutes in the J band and 60 minutes in the K_s band, with seeing of 0.″7 and 0.″6, respectively. We reduced the data with the IRAF DIMSUM package, following standard procedures. We barely detect the optical counterpart in the J band image at a magnitude of $J = 21.90 \pm 0.20$ but we do not detect it in the K_s image, which reached a magnitude limit of $K_s < 19.95$ (5 σ).

[13] IRAF is distributed by the National Optical Astronomy Observatory, which is operated by the Association of Universities for Research in Astronomy, Inc., under cooperative agreement with the National Science Foundation.

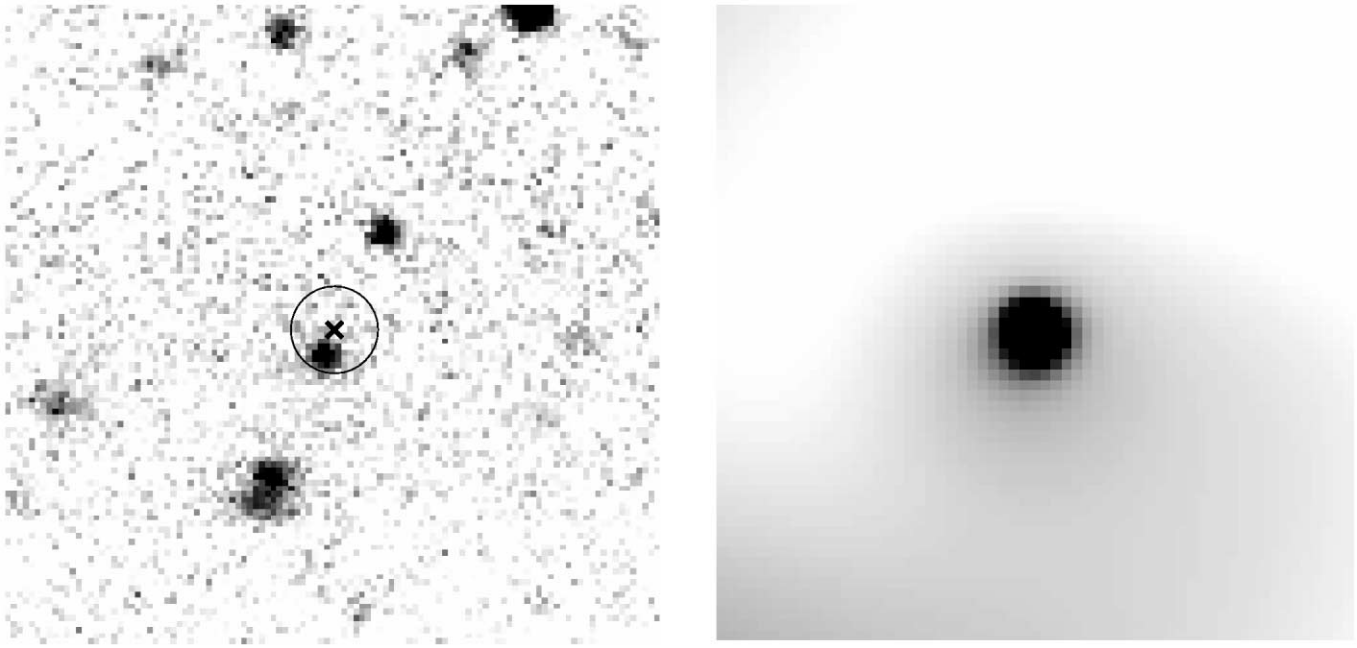

FIG. 2.—V and X-ray images of CXOCY J125304.0−090737. Both images are cutouts of $30'' \times 30''$ of the original images centered on the right ascension and declination of the X-ray source. North is up, and east to the left, in both images. The V image (*left*) was taken at the CTIO 4 m mosaic in a total exposure of 1 hr 20 minutes. The cross indicates the position of the X-ray centroid. A 2″ radius circle is also plotted. The X-ray image (*right*) was taken with the *Chandra* X-ray satellite with the ACIS-S chip S3, exposure time 49 ks. The X-ray image corresponds to the full (0.5–8 keV) band and has been adaptively smoothed using the CSMOOTH routine within CIAO. We apply a Gaussian kernel to the data and use an FFT convolution. The resulting image pixels are required to have a minimum significance of 3 σ and a maximum significance of 5 σ.

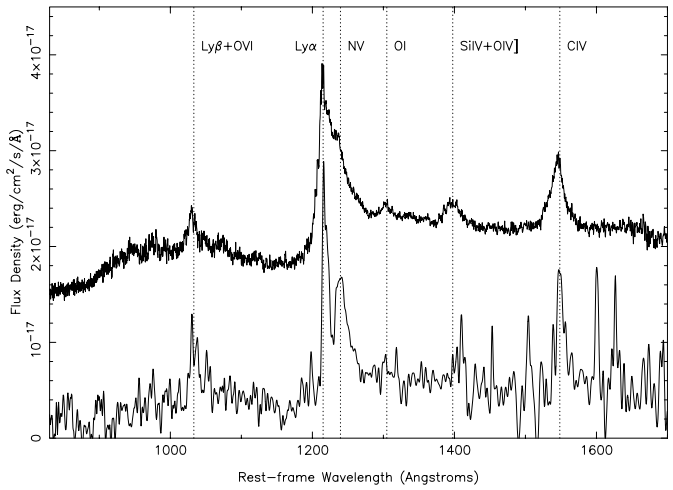

FIG. 3.—Optical spectrum of CXOCY J125304.0−090737 obtained at UT4/Yepun VLT. The spectrum has been smoothed in logarithmic space with a Gaussian of 250 km s^{-1}, equal to the spectral resolution of the instrument for the setup used, $R \sim 520$ ($v \sim 250$ km s^{-1}). For comparison we also show the error-weighted average of the SDSS Early Data Release QSO spectra at $z > 4$. Each individual spectrum used in the $z > 4$ composite spectrum has a resolution of $R \sim 1800$ ($v \sim 70$ km s^{-1}). This composite spectrum has arbitrary zero point and scaling offsets for display purposes, and it is shown above the spectrum of CXOCY J125304.0−090737. The most common QSO emission lines are indicated as dotted lines. The emission lines in CXOCY J125304.0−090737 are narrower than the typical SDSS spectrum.

2.3. *Optical Spectroscopy*

Follow-up spectroscopy of this field was obtained at the ESO Cerro Paranal Observatory with the UT4 Yepun telescope, using the FORS2/MXU instrument on 2002 February 14. Three masks were designed for the HCG62 field, one of which included a slit for the CXOCY J125304.0−090737 optical counterpart. We took three exposures with this mask for a total integration time of 1 hr 55 minutes in ∼0″.9 seeing conditions. We used the V300 grism, giving a resolution of $R \sim 520$ (10.5 Å) for our 1″ slit. The spectrum was reduced using standard techniques with IRAF and calibrated in wavelength using He-Ar comparison lamps exposures and the night sky lines. We also obtained spectra of the spectrophotometric standards Feige 67 and LTT 6248, which were used to provide a rough flux calibration of the spectrum.

Figure 3 shows the final spectrum together with the mean spectrum of quasars at $z > 4$ found in the SDSS. The typical broad emission lines of a quasar are clearly distinguishable and marked in the figure. We measure a mean redshift of $z = 4.179 \pm 0.006$, using all the emission lines but Lyα and N v.

3. DISCUSSION

Table 1 presents the observed properties of CXOCY J125304.0−090737. In the optical CXOCY J125304.0−090737 is a faint quasar with an absolute magnitude $M_{1450(1+z)} = -23.31 + 5 \times \log(h_{65})$ and $M_B = -23.69 + 5 \times \log(h_{65})$. At this absolute magnitude one would expect that most of the observed flux is coming from the QSO itself, with little contribution from its host galaxy, which is not resolved in our optical images. Its spectrum is typical of a quasar with broad emission lines (Fig. 3). We measure a velocity width of 1500 ± 300 km s^{-1} using the C IV emission line, which is lower than the one measured in the SDSS composite QSO spectrum (∼2800 km s^{-1}). On the other hand, the C IV rest-frame equivalent width (EW = 43 ± 10 Å) is larger than the SDSS QSO composite spectrum (∼24 Å), as expected from the Baldwin effect, an anticorrelation between 1450 Å luminosity and C IV EW (Baldwin et al. 1977). The spectrum also presents a strong absorption feature between the Lyα and N V emission lines. This feature is at approximately the same wavelength as the [O I] λ6364 sky line, and therefore its real strength is difficult to estimate. We are nevertheless confident that the absorption is real and not an artifact of the sky subtraction. We interpret this absorption line as intrinsic absorption of N V. It is approximately at 3000 km s^{-1} blueward of the emission line. Although the spectrum is noisy, one may tentatively argue that there are also absorption lines blueward of C IV and O VI at approximately the same velocity offset. If this were correct, it would imply the existence of material that could obscure the QSO. Another interpretation would be that the Lyα emission line is narrow and that we are seeing the trough between emission lines, although the wide red tail of N V would disfavor this hypothesis. The Lyα flux deficit, D_A, is a measure of the absorbed flux blueward of Lyα (Oke & Korycansky 1982; Schneider et al. 1991). We obtain a value of $D_A \sim 0.46$ for CXOCY J125304.0−090737, which is typical of quasars at this redshift (e.g., Madau 1995). Our measurement is only approximate because of the difficulty of fitting the continuum redward of Lyα in our poor signal-to-noise spectrum, which translates into a large uncertainty in the extrapolation of the continuum blueward to compute D_A.

Using our photometry, we measure a $V-I = 1.13$ color for CXOCY J125304.0−090737. This value is slightly bluer than the expected $V-I = 1.36$ color obtained redshifting the SDSS composite spectrum (Vanden Berk et al. 2001) and convolving the spectrum with the filter responses. The similarity between these values argues against large

TABLE 1
SUMMARY OF OBSERVED PROPERTIES OF CXOCY J125304.0−090737

Parameter	Value
R.A. (J2000.0)	12 53 04.0
Decl. (J2000.0)	−09 07 37
N_H[a]	2.96×10^{20} cm^{-2}
z	4.179 ± 0.006
α_{OX}	$\alpha_{ox} = -1.35^{+0.11}_{-0.13}$
V mag (Vega)	23.65 ± 0.05
I mag (Vega)	22.52 ± 0.08
J mag (Vega)	21.9 ± 0.2
K_s mag (Vega)	>20.5
M_I	$-23.45 + 5 \times \log(h_{65})$
$AB_{1450(1+z)}$	22.95 ± 0.10
$M_{1450(1+z)}$	$-23.0 + 5 \times \log(h_{65})$
f_X (0.5–8 keV)	$4.9 \pm 1.3 \times 10^{-15}$ ergs s^{-1} cm^{-2}
f_X (0.5–2 keV)	$1.7 \pm 0.4 \times 10^{-15}$ ergs s^{-1} cm^{-2}
f_X (2.0–8 keV)	$3.2 \pm 1.0 \times 10^{-15}$ ergs s^{-1} cm^{-2}
Hardness ratio	$-0.35^{+0.28}_{-0.25}$

NOTE.—Units of right ascension are hours, minutes, and seconds, and units of declination are degrees, arcminutes, and arcseconds.
[a] Calculated using HEASARC tool NH.

amounts of intrinsic reddening (and thus optical extinction) in CXOCY J125304.0−090737. However, this argument is only qualitative and does not exclude small amounts of extinction. Overall, considering the possible relatively weak intrinsic absorption lines in our spectrum of CXOCY J125304.0−090737 and its not very red photometric properties, we conclude that there may be small amounts of extinction in CXOCY J125304.0−090737.

In X-rays CXOCY J125304.0−090737 is also a faint QSO. The number of detected photons is low, 17.1 ± 4.2 in the soft (0.5–2.0 keV) band and 8.3 ± 3.0 in the hard (2.0–8.0 keV) band, and therefore fitting a power-law spectrum to the observed counts is difficult (see Fig. 1). Nevertheless, the best photon index slope is $\Gamma = 1.69^{+0.40}_{-0.35}$, which is harder than the average radio-quiet QSO X-ray spectrum at low redshift (Yuan et al. 1998; George et al. 2000; Mineo et al. 2000; Reeves & Turner 2000) (although part of the difference may be due to selection biases) and similar to the value of the X-ray background spectrum, $\Gamma \sim 1.4$ (e.g., Gendreau et al. 1995; Gilli et al. 2001). We have used this value ($\Gamma = 1.69$) to convert from observed count rate to X-ray flux. We measure an extinction-corrected X-ray flux of $4.9 \pm 0.5 \times 10^{-15}$ ergs cm^{-2} s^{-1} in the observed frame (0.5–8.0 keV) band. This QSO is therefore the second faintest X-ray–selected quasar detected so far (see Fig. 4) and the fourth X-ray–faintest high-redshift quasar overall.

For spectra with a low number of counts it is customary to characterize the spectral shape with the hardness ratio $\mathrm{HR} = (H - S)/(H + S)$, where S is the counts measured in a soft band and H is the counts in a hard band. The measured hardness ratio for CXOCY J125304.0−090737 is $-0.35^{+0.28}_{-0.25}$, defining the soft and hard X-ray bands as 0.5–2.0 keV and 2.0–8.0 keV, respectively. Although not many high-redshift quasars have measured hardness ratios in the literature, the ones measured are typically softer than ours. That is, their HRs are lower and their Γs are higher. Vignali et al. (2002d) measure a typical value of $\Gamma \simeq 2.0 \pm 0.2$, compared with our $\Gamma \sim 1.7$, emphasizing the relative hardness of CXOCY J125304.0−090737 compared with other optically selected high-redshift QSOs.

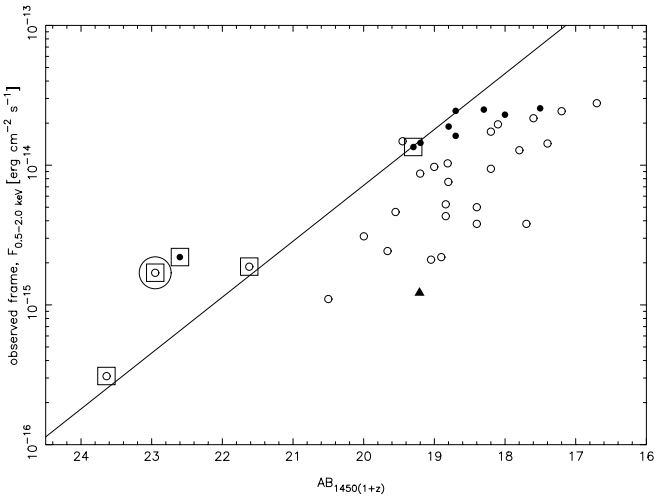

FIG. 4.—Soft X-ray flux (0.5–2 keV) vs. $AB_{1450(1+z)}$. Filled circles are *ROSAT* detections, empty circles are *Chandra* detections, and the filled triangle is the only *XMM-Newton* detection. Squares enclosing circles represent X-ray selection, while no enclosing sign denotes optical selection. CXOCY J125304.0−090737 is emphasized with another large concentric empty circle at $AB_{1450(1+z)} = 22.95$. Note that there are no optically selected QSOs detected in X-rays fainter than $AB_{1450(1+z)} \sim 20.5$. The solid line represents the locus of objects with $\alpha_{ox} = -1.5$ at $z = 4.5$ (see Fig. 5).

At redshifts $z > 4$ the observed *Chandra* band 0.5–8.0 keV corresponds to a rest-frame band of 2.5–40 keV or higher. Any process changing the observed spectral slope is thus occurring at intrinsic higher energies than observed. Strong intrinsic absorption can certainly harden an observed X-ray spectrum. At redshift $z > 4$, hydrogen column densities of $N_H \gtrsim 10^{23}$ are needed to produce noticeable spectral changes. In the case of CXOCY J125304.0−090737 neither the X-ray spectrum (Fig. 1) nor the optical one (Fig. 3) show any signs of such amounts of absorption. Processes such as Compton reflection (e.g., Guilbert & Rees 1988), which cause deviations from a power-law spectrum at high energies, may therefore be important for understanding the X-ray spectral properties of high-redshift quasars with hard spectra. The most prominent such features are iron emission lines, typically seen at 6.4 keV (from a neutral accretion disk) or 6.7 keV (from an ionized disk), iron absorption edges seen between 7.0 and 9.0 keV (with the energy again depending on the level of ionization in the disk), and a broad bump, typically between 30 and 50 keV, due to the Compton down-scattering of the high-energy photons. For typical parameters the spectrum of a $z = 4.19$ quasar can be hardened by 0.10–0.15 in Γ with respect to the underlying power law by the reflection component. The effects of reflection components on the X-ray background have been studied in more detail in past work (e.g., Fabian et al. 1990; Zdziarski et al. 1993).

In order to compare the optical and X-ray emission, we compute the effective optical to X-ray power-law spectral slope, α_{ox}, defined as

$$\alpha_{ox} = \frac{\log[f_\nu(2\ \mathrm{keV})/f_\nu(2500\ \text{Å})]}{\log[\nu(2\ \mathrm{keV})/\nu(2500\ \text{Å})]}\ , \qquad (1)$$

where f_ν is the flux density and ν is the frequency of the given wavelength or energy. Neither flux density is measured at the given energy and wavelength, and extrapolations are needed to compute this quantity. For CXOCY J125304.0−090737 we compute $\alpha_{ox} = -1.35^{+0.11}_{-0.13}$, taking into account the error in the measured quantities and the errors in the extrapolations.

We have also computed α_{ox} for all high-redshift quasars ($z > 4$) with measured $AB_{1450(1+z)}$ optical magnitudes and observed-frame 0.5–2.0 keV X-ray fluxes available in the literature. Figure 5 plots α_{ox} against the optical magnitude $AB_{1450(1+z)}$. The α_{ox} values of the X-ray–selected QSOs are shallower (X-ray stronger and/or optically fainter) than the optically selected ones. A Kolmogorov-Smirnov (KS) test indicates that the probability of both distributions being drawn from the same parent distribution is less than 0.05%. The distribution of optical absolute magnitudes (or luminosities) is also statistically different in the X-ray and optically selected samples, because the X-ray surveys are more sensitive but cover a much smaller area than the optical ones (see Figs. 4 and 6). In order to understand the difference in the α_{ox} values, we plot the X-ray against the rest-frame UV luminosity densities in Figure 6. We find that both observables are correlated with a functional form $L_{2\ \mathrm{keV}} \propto L^{0.55}_{1450\ \text{Å}}$, shown as a dashed line in Figure 6. This slope is somewhat shallower than that found by Vignali et al. (2002b). But taking into account that the faint UV luminosity points driving

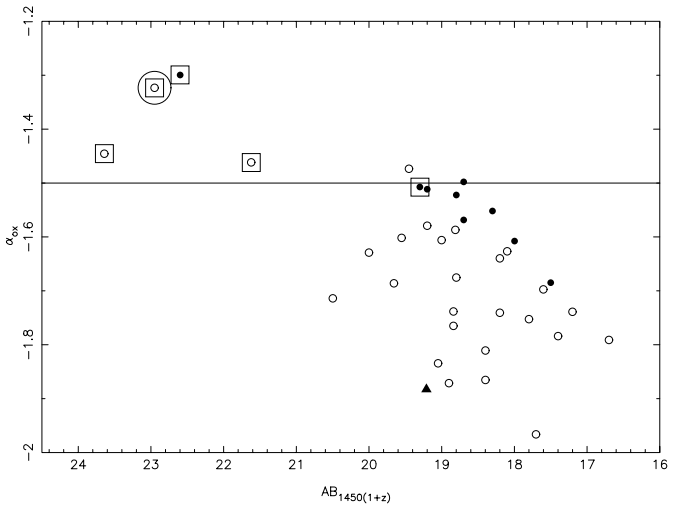

FIG. 5.—Plot of α_{OX} vs. $AB_{1450(1+z)}$. Symbols are as in Fig. 4. Small symbols denote detection: *ROSAT*, filled circle; *Chandra*, open circle; *XMM-Newton*, filled triangle. Large symbols denote selection: X-ray: square; optical: none. CXOCY J125304.0−090737 is highlighted with an extra large empty circle at $AB_{1450(1+z)} = 22.95$. The value of $\alpha_{ox} = -1.5$ is shown with a straight line. All optically selected QSOs have α_{ox} values lower than −1.46.

a shallower slope are X-ray–selected and assuming that the distribution of X-ray luminosities are the same at faint UV rest frame luminosities as at bright UV luminosities, our data are consistent with the correlation found by Vignali et al. (2002b), thus extending their result to fainter luminosities at high redshift with a larger sample.

CXOCY J125304.0−090737 was discovered in the first *Chandra* X-ray southern field studied within the CYDER survey. One can ask how many high-redshift QSOs one would expect to detect given the QSO luminosity function. We use Fan et al. (2001a) QSO optical luminosity function (LF), which is consistent with previous estimates (e.g., Kennefick et al. 1995; Schmidt et al. 1995). They compute the optically selected QSO LF in the range $3.6 < z < 5.0$ and $-27.75 < M_{1450} - 5 \times \log(h_{65}) < -25.75$. The optical

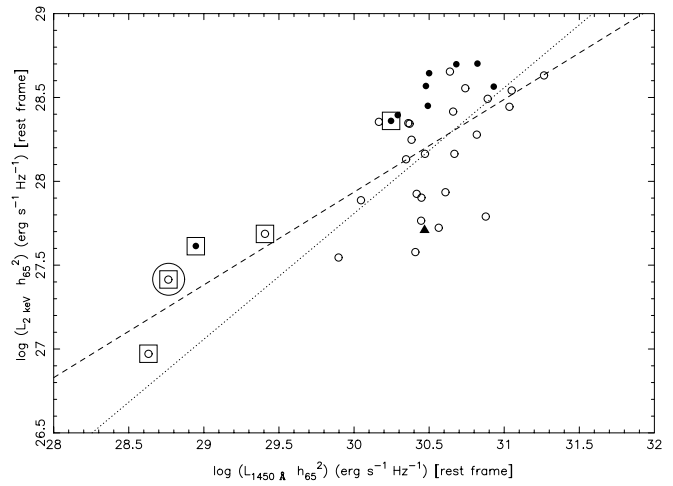

FIG. 6.—X-ray vs. optical luminosity densities. Symbols are the same as in Figs. 4 and 5. The dashed line is the best-fit linear regression including all points, which gives a slope of 0.55. The dotted line is a fit to the optically selected QSOs, fixing the slope at 0.75, as found by Vignali et al. (2002b).

absolute magnitude of CXOCY J125304.0−090737 is considerably fainter. If we extrapolate Fan et al.'s power-law LF down to the magnitudes reached by our search, the expected number of quasars in the ACIS-S S3 CCD with $z > 4$ is 0.22. The probability of finding *any* quasars (one or more) is then 20%. If instead we extrapolate Fan et al.'s LF to fainter luminosities, using the shape of the optical QSO LF at lower redshifts (Boyle et al. 2000), the expected number of QSOs is even lower. While, with just one detection, these numbers are not significant, they are nevertheless indicative that the faint end slope of the QSO optical LF may be high (at least higher than at low redshift) or that optical surveys miss significant fractions of QSOs that may be obscured. In the case of CXOCY J125304.0−090737 it is worth pointing out that its colors are typical of low-redshift quasars and therefore a multiwavelength optical survey reaching this magnitude limit should have been able to pick it up.

The number of expected $z > 4$ quasars can also be computed from the X-ray luminosity function (XLF). Unfortunately, the XLF is poorly determined above $z = 4$, given the lack of X-ray–selected QSOs at these redshifts. Compiling several X-ray surveys, Miyaji et al. (2001) derive an XLF up to $z = 4.6$, although at their highest redshift their XLF is only valid at the bright end. If we extrapolate their power-law parameterization of their last redshift bin ($z = 2.3$–4.6) to the faint end and also assume that the XLF is the same beyond $z = 4.6$, then we would expect to detect 0.72 quasars at the X-ray flux limit reached in our first CYDER field. If we instead extrapolate Miyaji et al's XLF with a smooth double power law to the faint end similar to the one at lower redshifts and also extrapolate this function to higher redshift with a plausible evolutionary model (see Castander et al. 2003 for details), we obtain somewhat lower expectation values. The probability of finding any quasars would then be $\lesssim 50\%$. We want to stress nevertheless that these numbers should be taken cautiously. They are only for orientation, to give a sense of how the faint end of the high-redshift quasar luminosity function may behave.

The discovery of CXOCY J125304.0−090737, together with the other X-ray–selected high-redshift QSOs (Henry et al. 1994; Zickgraf et al. 1997; Schneider et al. 1998; Silverman et al. 2002; Barger et al. 2002), demonstrates the potential of X-ray techniques to detect high-redshift QSOs. At redshifts $z > 4$, X-ray photons observed, for example, at 1 keV, were emitted at energies greater than 5 keV, where the X-ray photons can penetrate even considerable amounts of extinction and therefore X-ray–selected samples should be almost free of extinction bias. Only sources with intrinsic column densities $N_H \gtrsim 10^{23}$ cm^2 should be affected. In particular, *Chandra,* with its superior image quality that allows secure and economical identifications of optical counterparts, will permit the completion of follow-up surveys, some of which are already in progress, such as the CYDER survey, which augur a new understanding of the quasar population at high redshift. For example, one can argue that one needs of the order of 100 high-redshift quasars to constrain the high-redshift LF. This could be achieved with 40–200 *Chandra* pointings (ACIS-I and ACIS-S), depending on whether the actual QSOs LF at the faint end is as our discovery implies or lower. Although demanding, current on-going X-ray follow-up surveys may achieve these numbers. These discoveries will be complemented by deep wide-field multiband optical

surveys to provide a good understanding of the high-redshift quasar population and thus the history of the accretion power onto black holes, which is thought to be closely related to the galaxy formation and star formation rate history of the universe.

4. CONCLUSIONS

We present the discovery of CXOCY J125304.0−090737, a new high-redshift quasar at $z = 4.179$ found as part of the CYDER survey. CXOCY J125304.0−090737 is an optically faint quasar [$M_B = -23.69 + 5 \times \log(h_{65})$] with a typical QSO spectrum (Fig. 3). In the optical the quasar seems to be slightly obscured, although the data are also consistent with no extinction. In X-rays CXOCY J125304.0−090737 is also X-ray faint ($f_X = 1.7 \pm 0.4 \times 10^{-15}$ ergs s^{-1} cm^{-2} in the 0.5–2.0 keV band) with a somewhat harder spectrum ($\Gamma \sim 1.7$ or HR ~ -0.35) than typical low- or high-redshift optically selected quasars. We speculate that a reflection component can slightly harden the spectrum, but by no means is this the only mechanism. The spectrum of CXOCY J125304.0−090737 and the other X-ray–selected high-redshift quasars is X-ray strong (and/or optically weak) compared with high-redshift optically selected quasars. Given that both samples have different optical/ultraviolet absolute magnitudes, this result is a manifestation of the correlation between X-ray and rest-frame ultraviolet luminosities. Taking into account selection biases, we find a slope for this correlation consistent with the value obtained by Vignali et al. (2002b). We therefore extend their result to lower luminosities at high redshifts using a larger sample.

The quasar space density implied by the discovery of CXOCY J125304.0−090737 is high: a factor $\gtrsim 5$ larger than reasonable extrapolations of the quasar optical luminosity function at high redshift. Although not statistically significant, this number seems to indicate that the shape of the quasar luminosity is changing, with the faint-end slope becoming steeper with redshift, or that current optical surveys at high redshift are missing considerable numbers of quasars. The space density predicted from the X-ray luminosity function is more a guess than a prediction. Anyway, if on-going and future X-ray surveys corroborate the numbers implied by the first field of the CYDER survey, the X-ray luminosity function will not differ much from its value at lower redshifts, $z = 2$–3. The combination of the currently ongoing optical and X-ray surveys with complementary regions of the parameter space sampled will help to determine the quasar luminosity function at high redshift with a better understanding of the biases involved with both selections. The CYDER survey promises to be one of the contributors to a better understanding of the quasar population at high redshift.

The CYDER survey participants, and especially F. J. C. and E. T., acknowledge support from the Fundación Andes. J. M. acknowledges support from FONDECYT.

REFERENCES

Anderson, S. F., et al. 2001, AJ, 122, 503
Baldwin, J. A. 1977, ApJ, 214, 679
Barger, A. J., et al. 2002, AJ, 124, 1839
Bechtold, J., et al. 2002, ApJ, in press
Bennett, A. S. 1962, MmRAS, 68, 163
Boyle, B. J., et al. 2000, MNRAS, 317, 1014
Brandt W. N., et al. 2001, AJ, 122, 1
Brandt W. N., Schneider D. P., et al. 2002a, ApJ, 569, L5
Brandt W. N., Schneider D. P., Vignali, C., Fan, X., Kaspi, S., & Schneider, D. P. 2002b, in X-Ray Spectroscopy of AGN with *Chandra* and *XMM-Newton*, ed. T. Boller, S. Komossa, S. Kahn, H. Kunieda, & L. Gallo (Garching: MPE), 235
Castander, F. J., et al. 2003, in preparation
Castander, F. J., Treister, E., Maza, J., Coppi, P., Maccarone, T., Zepf, S., Guzmán, R., & Ruiz, M. T. 2003, Astron. Nachr., in press
Edge, D. O., Shakeshaft, J. R., McAdam, W. B., Baldwin, J. E., & Archer, S. 1959, MmRAS, 68, 37
Fabian, A. C., et al. 1990, MNRAS, 242, P14
Fan X., et al. 2001a, AJ, 121, 54
———. 2001b, AJ, 122, 2833
Gendreau, K. C., et al. 1995, PASJ, 47, L5
George, I. M., et al. 2000, ApJ, 531, 52
Gilli, R., Salvati, M., & Hasinger, G. 2001, A&A, 366, 407
Guilbert, P. W., & Rees, M. J. 1988, MNRAS, 233, 475
Henry, P. J., et al. 1994, AJ, 107, 1270
Kaspi, S., Brandt, W. N., & Schneider, D. P. 2000, AJ, 119, 2031
Kennefick, J. D., Djorgovski, S. G., & de Carvalho, R. R. 1995, AJ, 110, 2553
Madau, P. 1995, ApJ, 441, 18
Mineo, T., et al. 2000, A&A, 359, 471
Miyaji, T., Hasinger, G., & Schmidt, M. 2001, A&A, 369, 49
Oke, J. B., & Korykansky, D. G. 1982, ApJ, 255, 11
Reeves, J. N., & Turner, M. J. L. 2000, MNRAS, 316, 234
Richards, G. T., et al. 2003, AJ, submitted
Sandage, A. 1965, ApJ, 141, 1560
Schneider, D. P, et al. 1998, AJ, 115, 1230
———. 2002, AJ, 123, 567
Schneider, D. P., Schmidt, M., & Gunn, J. E. 1991, AJ, 101, 2004
Silverman, J. D., et al. 2002, ApJ, 569, L1
Schmidt, M. 1963, Nature, 197, 1040
Schmidt, M., Schneider, D. P., & Gunn, J. E. 1995, AJ, 110, 68
Treister, E., & Castander, F. J. 2003, Astron. Nachr., in press
Vanden Berk, D. E., et al. 2001, AJ, 122, 549
Vignali, C., Bauer, F. E., Alexander, D. M., Brandt, W. N., Hornschemeier, A. E., Schneider, D. P., & Garmire, G. P. 2002a, ApJ, 580, L105
Vignali, C., Brandt, W. N., Fan, X., Gunn, J. E., Kaspi, S., Schneider, D. P., & Strauss, M. A. 2001, AJ, 122, 2143
Vignali, C., Brandt, W. N., & Schneider, D. P. 2002b, AJ, 125, 433
Vignali, C., Brandt, W. N., Schneider, D. P., & Garmire, G. P. 2002c, Inflows, Outflows, and Reprocessing around Black Holes, (astro-ph/0210001)
Vignali, C., Brandt, W. N., Schneider, D. P., Garmire, G. P., & Kaspi, S. 2002d, AJ, 125, 418
White, R. L., et al. 2000, ApJS, 126, 133
York, D. G., et al. 2000, AJ, 120, 1579
Yuan, W., Brinkmann, W., Siefert, J., & Voges, W. 1998, A&A, 330, 108
Zdziarski, A. A., et al. 1993, ApJ, 405, 125
Zickgraf, F.-J., et al. 1997, A&A, 323, L21